

Quantum Coherence in Loopless Superconductive Networks

Massimiliano Lucci ^{1,†}, Valerio Campanari ², Davide Cassi ³, Vittorio Merlo ¹ , Francesco Romeo ⁴ , Gaetano Salina ⁵  and Matteo Cirillo ^{1,*}

¹ Dipartimento di Fisica and MINAS Lab, Università di Roma “Tor Vergata”, 00133 Roma, Italy

² Dipartimento di Elettronica, Università di Roma “Tor Vergata”, 00133 Roma, Italy

³ Dipartimento di Scienze Matematiche, Fisiche ed Informatiche, Università di Parma, 43124 Parma, Italy

⁴ Dipartimento di Fisica “E. R. Caianiello”, Università di Salerno, 84084 Fisciano, Italy

⁵ Istituto Nazionale di Fisica Nucleare, Sezione Roma Tor Vergata, 00133 Roma, Italy

* Correspondence: cirillo@roma2.infn.it; Tel.: +39-0672594518

† Passed away on 17 May 2022.

Abstract: Measurements indicating that planar networks of superconductive islands connected by Josephson junctions display long-range quantum coherence are reported. The networks consist of superconducting islands connected by Josephson junctions and have a tree-like topological structure containing no loops. Enhancements of superconductive gaps over specific branches of the networks and sharp increases in pair currents are the main signatures of the coherent states. In order to unambiguously attribute the observed effects to branches being embedded in the networks, comparisons with geometrically equivalent—but isolated—counterparts are reported. Tuning the Josephson coupling energy by an external magnetic field generates increases in the Josephson currents, along the above-mentioned specific branches, which follow a functional dependence typical of phase transitions. Results are presented for double comb and star geometry networks, and in both cases, the observed effects provide positive quantitative evidence of the predictions of existing theoretical models.

Keywords: macroscopic quantum coherence; superconductive tunneling; Josephson junction networks



Citation: Lucci, M.; Campanari, V.; Cassi, D.; Merlo, V.; Romeo, F.; Salina, G.; Cirillo, M. Quantum Coherence in Loopless Superconductive Networks. *Entropy* **2022**, *24*, 1690. <https://doi.org/10.3390/e24111690>

Academic Editors: Antonino Messina and Agostino Migliore

Received: 21 October 2022

Accepted: 16 November 2022

Published: 18 November 2022

Publisher’s Note: MDPI stays neutral with regard to jurisdictional claims in published maps and institutional affiliations.



Copyright: © 2022 by the authors. Licensee MDPI, Basel, Switzerland. This article is an open access article distributed under the terms and conditions of the Creative Commons Attribution (CC BY) license (<https://creativecommons.org/licenses/by/4.0/>).

1. Introduction

In 1979, it was proposed [1] that a Berezinski–Kosterlitz–Thouless (BKT) phase transition [2] in two-dimensional superconducting films could occur, and its possible evidence was linked to the sheet resistance of the films. Later, interest was raised in the possible observation of BKT transition on two-dimensional arrays of superconductive islands shaped to form closed loops when connected by Josephson junctions [3]. The evidence of the BKT transition of the arrays would be the activation, below a given temperature, of vortex–antivortex pairs and the resistive transitions accompanying their motion. The topic had noticeable developments in the early ’80s, but the 1986 discovery of High Tc Superconductors (HTCS) [4] caught most of the attention of the condensed matter community for understanding the properties of the cuprates. It was so that even the investigations of BKT and topological transitions in superconductors were somewhat put aside due to the wave of interest for high-Tc superconductivity research and perspectives. It is worth recalling that a BKT transition is a phenomenon predictable in superconductive systems only when the temperature of these stands safely below the superconducting transition temperatures. It is then understandable that the exceptional rises of these temperatures (up to 120 K at atmospheric pressure) of the new materials would primarily attract research work.

The development of laser cooling techniques in the mid-80s [5], and the consequent discovery of Bose-Einstein Condensation (BEC) in alkali atoms vapors in the mid-90s [6], raised a noticeable burst of activity related to the physics of systems described by macroscopic wavefunctions, and, within this framework, attention to BKT phenomenology and

topological phase transitions in condensed matter grew again [7]. Attempts to combine BEC physics and network connectivity have been provided, both from a theoretical physics [8] and mathematical [9,10] point of view. These efforts, analyzing populations of bosons distributed over the sites of discrete reticles having specific nearest neighbor connectivity (and adequate intra-sites coupling potentials), demonstrated that in these systems, peculiar long-range macroscopic wavefunction configuration and thermodynamic features typical of BEC transitions are possible. Although the theoretical predictions were first conceived for reticles of bosons of optical networks, attention was also dedicated [11] to the possibility that of same effects being observed in arrays of superconducting islands connected by Josephson junctions containing no superconductive loops: in this case, the role of the bosons on the reticles sites should be played by Cooper pairs. A strong argument in favor of this intuition comes from noting that the Bose–Hubbard model, under the macroscopic occupation of the lattice sites, implies a non-linear Schrodinger equation (NSE) for the condensate wavefunction. The NSE, in turn, can be organized in the form of a generalized Feynman’s model [12] describing the Josephson coupling among the lattice sites (superconducting islands). The aforementioned observation suggests a close analogy between the hopping of bosons in optical networks and Cooper pair dynamics on networks of superconducting islands coupled by the Josephson effect.

From an experimental point of view, to our knowledge, there has not been much activity dedicated to experimentally investigating the bosonic nature of Cooper pairs and, therefore, a probe of the predictions of [11], relying on Cooper pairs acting as hopping bosons, would constitute evidence of such an integer spin behavior. Besides the exposed analysis in terms of BEC, it is worth noting that a parallel between a BKT transition and the phenomena predicted in [11] exists: the “hopping” of bosons between all the islands of the superconductive arrays can generate a long-range correlation of the wave functions in the system only when the Josephson coupling energy is of the order or less than the thermal energy [11]. This is analogous to saying, in BKT language, that a long-range correlation leading to vortex–antivortex dissociation can exist only below a critical temperature.

The systems we herein investigate present a twofold topological aspect: the first concerns the spatial long-range coherence of macroscopic wavefunctions, a phenomenon nowadays addressed as “topological order”. The second comes from the fact that the “topological order” in the specific case can be achieved through specific node-to-node connections, which are the basis for the topological analyses of electrical networks and graph theory. We will show that the evidence of long-range order in our systems comes from both Josephson supercurrent peculiarities and gap increases of the islands of the discrete systems we investigate. It is herein shown, by new samples, new data, and more quantitative arguments, that previously observed effects on double comb [13,14] and star graph arrays of Josephson junctions [15,16] can be safely attributed to the peculiar topology (in terms of connectivity) of these structures.

2. Double Comb-Like Structures

In Figure 1, CAD designs of the superconducting networks whose features are investigated in our experiments are displayed. Figure 1a shows a portion of the backbone of a double comb planar array in which the “fingers” of the comb are just superconducting shorts. We call the backbone the linear array of islands from which the fingers depart. The arrows indicate the location of Josephson junctions (JJ).

In Figure 1b, we present a double comb structure having the fingers made of superconductive islands connected by Josephson junctions. Fingers are linear arrays connected to the backbone, above and below it. Each island of the backbone is connected to four neighboring islands, while islands belonging to the fingers are connected to two neighbors. All the superconductive islands have been designed to have in the final chip the same volume, which was possible due to the different thicknesses of the base and contact electrodes layers. Responsible for the connections between the islands are the Josephson junctions which are the ($3\ \mu\text{m} \times 3\ \mu\text{m}$) squares indicated by the arrows. The superconductive islands are made

in niobium, and the Josephson tunnel junctions are fabricated with Nb-NbAlO_x-Nb technology [17]. The backbone branch was formed by 101 superconductive islands, while each finger branch has 50 islands. The current–voltage (IV) characteristics of fingers have been measured by biasing two aligned fingers in series making a connection of 101 islands as well (notice that the extra island, connecting two aligned fingers, belongs to the backbone).

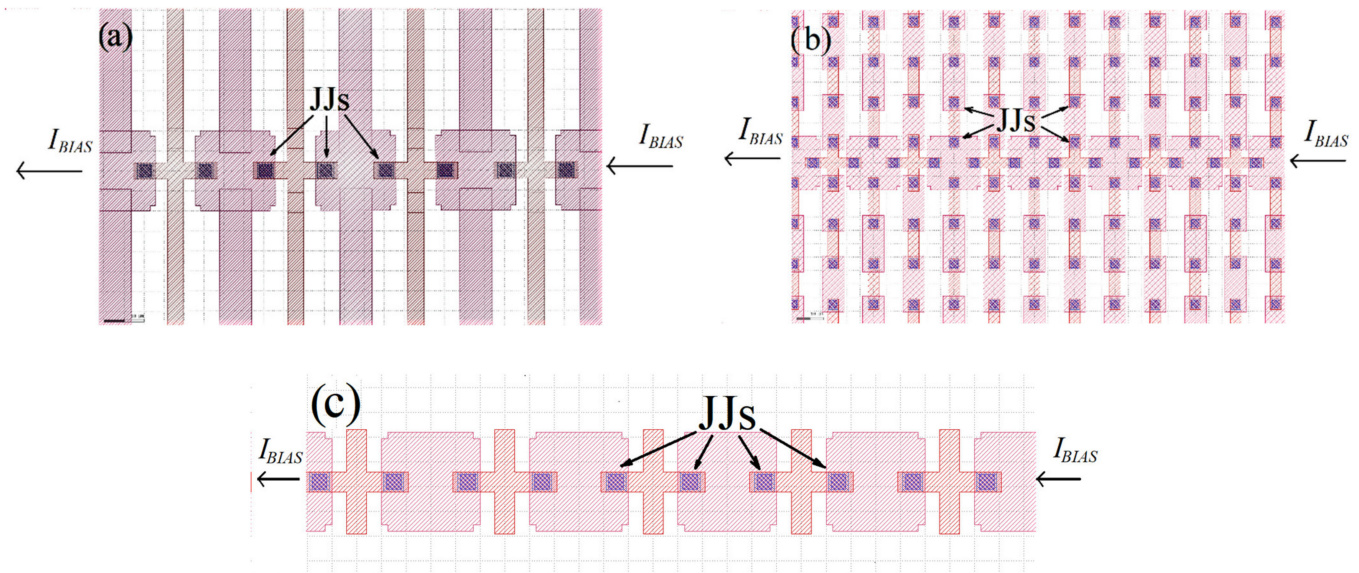


Figure 1. (a) Zoom of the backbone region of a double comb-like structure having long superconducting shorts (thin films) as fingers. In (b,c), we show, respectively, portions of the backbone region of a complete double comb array, with superconductive islands connected by Josephson junctions on the fingers, and of a reference backbone array, with no fingers. The latter has the same geometrical structure of the backbone arrays in (a,b). The JJs arrows in the figures indicate the locations of Josephson junctions; the direction of the bias current I_{BIAS} feeding the arrays is also indicated. An external magnetic field for these arrays is applied along the direction perpendicular to the bias current feeding line.

In Figure 1c, we show what we call a “reference” backbone array, namely a backbone array with no finger connections attached to it. It is worth noting that the superconducting “shorts” generating the fingers in Figure 1a are extensions, in alternate successions, of base or contact electrodes of the backbone islands and all have the same volume. Both reference and the “shorted-fingers” arrays were designed to perform comparative analyses with the current–voltage characteristics of the backbone array embedded in a graph structure (Figure 1b): the junctions connecting the backbone islands to the fingers are deliberately missing in Figure 1a,c in order to isolate geometrical from connectivity effects.

We will herein call SH (Shorts) the backbone array obtained by the serial connection along the backbone feeding line of Figure 1a, BB the same array obtained by the serial connection of the backbone of the double comb of Figure 1b, and BBR the serial connection (through Josephson junctions) obtained by the island of the reference array.

The IV characteristics we investigate are those obtained by biasing the arrays from four final contact pads (two to the left end and two to the right end), and we observe the voltage sum of 100 junctions in a typical four-probe configuration. In order to isolate the arrays from the final contact pads, we insert normal metal layers between the array’s ends and contact pads. In general, for the present design, $N + 1$ superconductive islands (including the two final “contact” islands) generate N junctions. The data we present herein were all obtained with the samples immersed in a ⁴He bath. The helium dewar was put inside a μ -metal cylinder, and an additional cryoperm shield surrounded the samples in the bath at 4.2 K. The current noise level for our combined analog/digital acquisition system is of the order of a few nanoamperes; the voltage signals generated at the “cold” end by the chips

are amplified at room temperature and fed to a data acquisition system. The “philosophy” behind our chip design is twofold: In the first stage, we investigate the IV curves of the backbone array in the presence (Figure 1b) or in the absence of granular fingers (as in Figure 1c). In the second stage we investigate the role played by the fingers granularity by modifying the network in Figure 1b to include fingers just made of a single superconducting film which does not include Josephson junction-connected islands (see Figure 1a).

A comparison between the three arrays of Figure 1 is shown in Figure 2. In Figure 2a, we see that the current–voltage characteristic of a backbone array has higher Josephson currents and higher gap-sum voltage with respect to the reference array, a result consistent with those reported in previous papers [13,14]. In this figure, however, we also show the current–voltage characteristics of the backbone array with superconducting shorts of Figure 1a. We can see that for this array, the Josephson currents are, up to 100 mV, equal to the currents of the backbone array, and after this voltage, the “shorted fingers” array has higher Josephson currents. Note that the sort of “grass” appearing on the switching distributions of the samples does not depend on the noise of the measurement apparatus, but it is an intrinsic characteristic of the junctions of the arrays having slight barrier/geometrical defects generating quasi-particle current dispersion which adds to the Josephson currents when measuring the series connection.

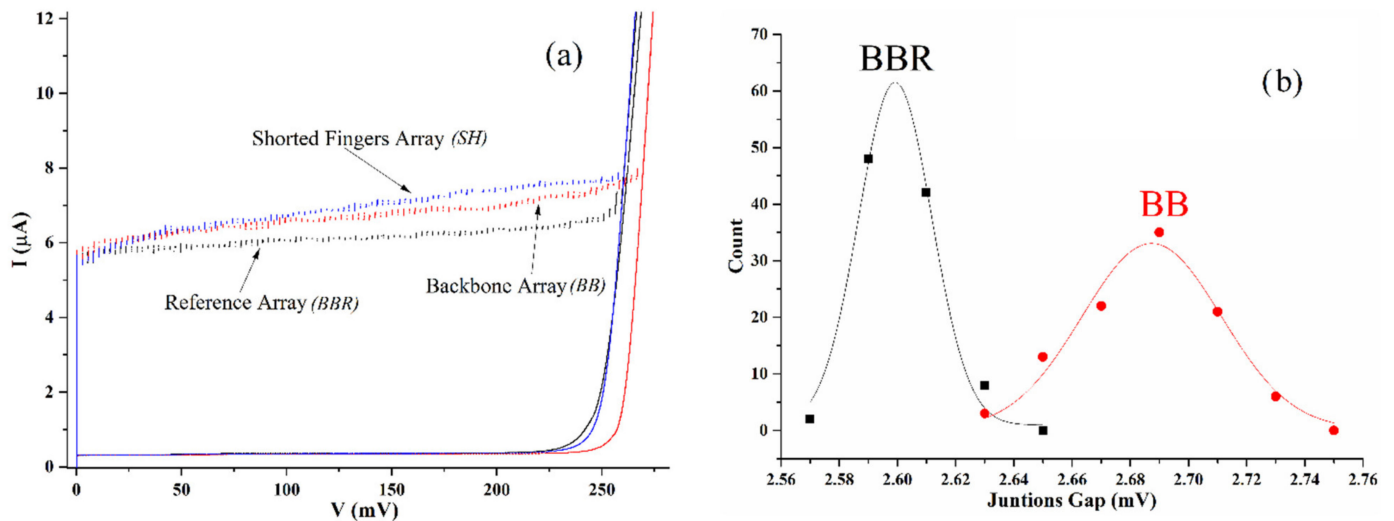


Figure 2. (a) Comparison of the current–voltage characteristic of the backbone array (red) of a complete comb structure with that of a “backbone reference array” (black) and “shorted-fingers array” (blue): we can see that the reference array has both Josephson currents and a gap-sum voltage less than those of the backbone array while the shorted finger has more than half of the Josephson currents higher than those of the backbone but the same gap-sum of the reference array; (b) statistical distribution of the superconducting gaps of the 100 junctions for reference (BBR) and backbone (BB) array. From the plot, we extract that a single gap voltage of an island of a backbone array is 3% higher than the reference backbone array.

It is important to point out that when tracing current–voltage characteristics, as we did for Figure 2a, the top of the Josephson currents (just before the switches from zero voltage occur) correspond to states in which the Josephson potential, coupling the current-biased junctions, becomes very low [18,19], while, for current unbiased junctions, lying on the fingers of the arrays, the Josephson energy is much higher than the energy of thermal fluctuations at 4.2 K (roughly a factor 30 for a maximum Josephson current of 5.6 μA). In these conditions, we might not fully exploit the characteristics of the phase transition predicted in [11], but the observed effects show that (i) the fingers in a double comb structure are necessary to observe the increase of the Josephson currents; and (ii) the increase we observe is, over roughly 15% of the junctions of the backbone array, of the same order of what one could observe if the fingers arrays were to be replaced by a single

superconducting short. In other terms, (i) and (ii) provide evidence that the effect of the finger branches is equivalent to that of a single superconducting film (described by a single wavefunction) as far as the amplitude of Josephson critical currents is concerned.

We suppose that above 100 mV, the backbone array currents of the complete comb (Figure 1b) are smaller than those of the shorted-fingers array (Figure 1a) since, as discussed above, the Josephson energy for the unbiased junctions of the fingers is too high with respect to thermal fluctuations that can generate hopping and charge migration between islands. For reasons that will be clear in a few paragraphs below, we believe that is a rather reasonable explanation for the difference.

In Figure 2b, we have plotted the normalized distribution of the gap amplitudes of all the junctions of the backbone and reference array of one chip. We can see that the distributions are mostly gaussian (the curve through the data) and that the peak of the backbone array is 3% ahead of the peak of the reference array. The information coming from these distributions suggests that the junctions of the backbone array have a gap increase distributed around a mean value, and this is solid evidence of a regular increase of the superconducting gap (and condensation energy) all over the islands of the array. The average value of the distributions returned by the fits are, respectively, (2.687 ± 0.005) mV for the backbone array and (2.599 ± 0.003) mV for the reference, where the error is relative to the standard error of the mean $\bar{\sigma} = \sigma/\sqrt{N}$ where σ is the standard deviation to be associated with each measurement, and N is the number of gaps measured (100). We note that the statistical errors are at least one order of magnitude larger than the instrumental errors which range in the order of tens or hundreds of nanovolts of magnitude. The plot of Figure 2b was obtained by grouping the 100 gap readings in intervals of 20 μ V. A Student unpaired t-test over all the data (100 for each curve) relative to the gaussian curves in Figure 2b showed as a result that the probability of the difference of the means being caused by statistical fluctuations is less than 10^{-4} .

In terms of the gap dependence on the temperature [18], the observed gap difference would correspond, at 4.2 K, to a temperature difference of 0.8 K between the two arrays. The backbone array then should be “colder” than the reference array of 0.8 K: this effect is not attributed to “fingers cooling”, em-antenna effects or anything else since the gaps of backbone arrays with the shorted fingers (SH) (Figure 1a) have the same values of the reference array (BBR). It is also worth recalling that we are measuring in a liquid helium bath and such thermal gradients are not really conceivable for samples dissipating a few microwatts of power and are less than a millimeter apart on the same chip (the latent heat of evaporation of ^4He , at atmospheric pressure, is 21 kJ/kg). Thus, the increased gaps of the junctions on the BB array have to be uniquely attributed to the specific topology (in terms of connectivity) and, in particular, to having “granular” fingers attached to the backbone. Figure 2b shows that the statistical distribution of the gaps has a gaussian shape just like that of the geometrically equivalent array, meaning that, apart from the statistical fluctuations, a uniform increase of the gap is distributed all over the backbone islands. It must be noted that in Figure 2b, the distribution of the data (collected using the same “voltage bins” for the statistical analysis) is wider for the backbone array meaning that the gap increase on the backbone has a higher disuniformity. We will show in the next paragraph that this dispersion depends on finite size effects on the comb for which the gap increase tends to be reduced at the ends of the structure.

In Figure 3a, we show the gap increase of the central finger, CF, (meaning the series connection of two aligned fingers) located in the center of the comb structure (red) with respect to the very last finger LF (black). Here, we can see that the central finger array has a gap-sum voltage higher than the one of the last finger. In Figure 3b, where we show the statistical distribution of the gaps along the central and last fingers, we can see the difference between the central peaks of reference and the lateral array. In particular, the mean gap value of the central finger is (2.675 ± 0.004) mV while the mean of the last finger is (2.641 ± 0.008) mV. Here again, the plot was obtained by grouping the data in intervals of 30 μ V and a Student’s unpaired t-test performed on all the available gaps

(100 for each array) provides a rather high confidence that the observed differences between the two means cannot be generated by statistical fluctuations (the contrary has a probability less than 10^{-4}). Physically, the two distributions tell us that there is a difference as we move along the backbone toward the physical ends of the double comb structure and, therefore, it is reasonable to expect, as we mentioned before, a wider distribution of an embedded backbone array with respect to its geometrical equivalent as we see in Figure 2b. In Figure 3b, we see that, besides having the central peak for a higher value of the voltage, the distribution of the central finger array is even more peaked than that of the lateral array, meaning that there is more coherence (in terms of uniform increase) of the gap values along the central finger which is deeply embedded in the double comb structure.

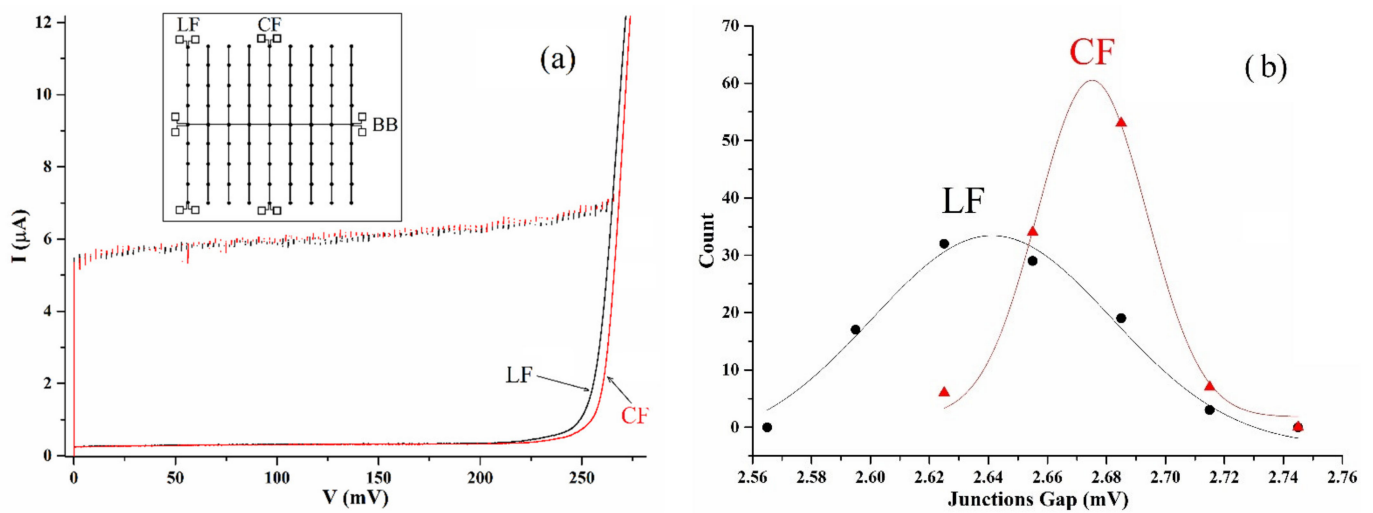


Figure 3. (a) The current–voltage characteristics of central finger (red) and last finger (black); (b) the statistical distributions of the gaps of lateral finger (LF) and central finger (CF). We can clearly see the finite size effect of the comb structure through the gap increase of the central finger with respect to the lateral finger.

Hereafter, we present a comparison between the magnetic field behavior of the arrays of Figure 1 by applying an external field. The magnetic field, generated by a superconducting niobium solenoid, has a direction lying in the planes of the arrays perpendicular to the backbone arrays lines, i.e., parallel to the fingers. The field depresses uniformly all Josephson junction critical currents I_c of the junctions of the arrays, and related coupling energies $\Phi_0 I_c / 2\pi$, through the Fraunhofer pattern and, therefore, any thermal effect due to the flipping of Cooper pairs between the islands can be enhanced. In Figure 4a, we show the dependence of the difference ΔI between average Josephson currents of the backbone array and reference array averaged in the interval (100–150) mV. The difference is normalized to the value of the average reference current at each specific magnetic field value and, therefore, what we measure is the relative percentage of the increase in the Josephson current of the backbone array $\frac{\Delta I}{I(B)} = \frac{const}{\sqrt{B_c - B}}$. We see that, when the magnetic field is around 27.5 G, a sharp increase of the percentage takes over (see inset where the abrupt increase is evident) up to the point that the average currents of the backbone become more than three times that of the reference array. The curve we just wrote is a typical phase-transition dependency describing the experimental points with a coefficient of determination (R^2) different from the unity only for four parts over 10^4 ; the experimental error bars are essentially unimportant for the fit since all the experimental data are intercepted by the theoretical curve. In any case, the maximum uncertainty to be associated with the points of the plot is of the order of 15% (due to the averaging of the values). Additionally, right after the maximum, the data attain a zero value because we are not far from the first minimum of the Josephson current which occurs for $B = 30$ G and, therefore, the static vortex trapped in each

junction substantially changes the static distribution of the phase and sets the Josephson currents to zero.

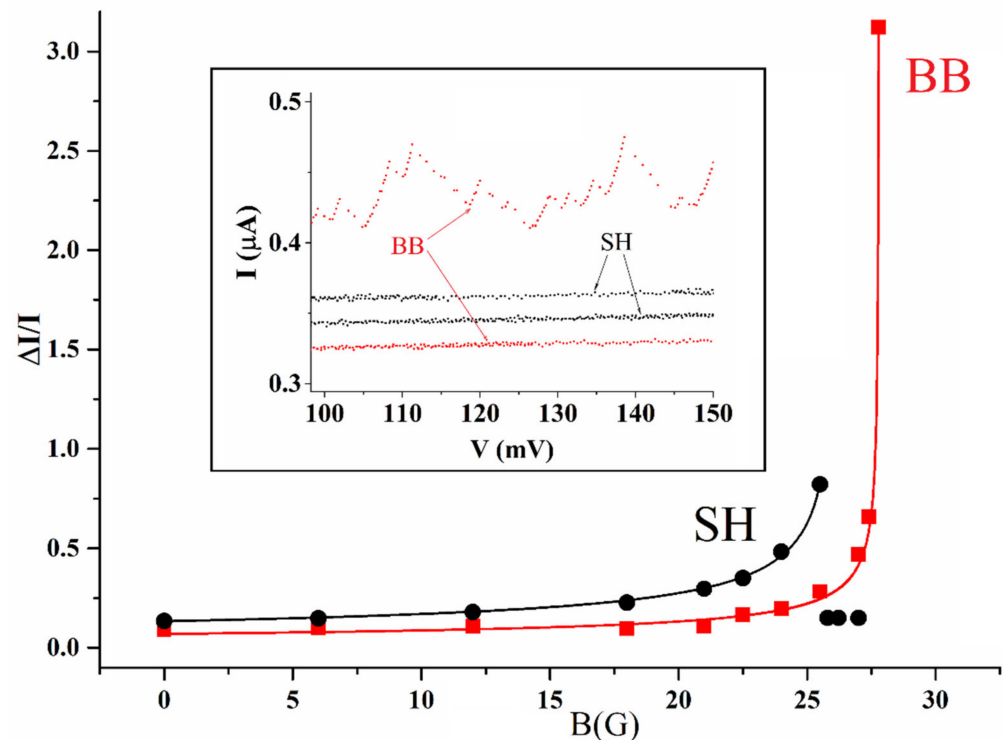


Figure 4. The red squares show the relative average increase (ΔI) of the Josephson critical currents of the BB array of the complete double comb (Figure 1b) with respect to that (BBR) of the reference array (Figure 1c) measured for increasing values of an applied external magnetic field. The relative increase is normalized to the average current of the reference array for each field: we can see that for a field value of $B = 27.5$ G, the average Josephson current of the backbone array is more than three times higher than the currents of the reference array (as visible in the inset). The black circles show the dependence of the difference between the average Josephson critical current heights of SH and BBR arrays: in this case, we can see that there are no sharp increases like for the black squares. This effect is also visually illustrated in the inset where we see that the “shorted fingers” array currents remain much lower than the values attained by the backbone of the complete comb structure.

In Figure 4, we also show the results obtained now measuring the magnetic field response of the shorted-finger array. In this case, we can see a much more limited increase of the Josephson currents of the short-finger array backbone with respect to the reference backbone array. The latter observation implies that the sharp increase we observe in Figure 4 is generated by the granularity of the finger array made of coupled superconductive islands. In the zero applied field, for a maximum Josephson current of $5.6 \mu\text{A}$, the Josephson coupling energy is roughly 30 times higher than the thermal energy at 4.2 K (5.8×10^{-23} J).

However, at the field of 27 G, the average Josephson current of the reference array is $0.270 \mu\text{A}$ which leads to a Josephson zero-bias energy of 8.9×10^{-23} J, a bit above the thermal energy written before and, therefore, thermal hopping is possible all over the islands of the comb array causing a sharp increase of the Josephson currents of the backbone. Thus, the behavior under the applied magnetic field of the three arrays shows, unambiguously, that the observed current increases in the backbone array embedded in the double comb structure are due to a macroscopic transition in the sense exposed in [11]: when the Josephson coupling energy between the islands becomes of the order of the thermal energy, the migration of pairs from the fingers toward the islands of the backbone increases sharply, leading to a noticeable increase of the Josephson currents. On the fingers of the shorted finger arrays, we do not have the gradient of charge carriers

generated by Josephson energy modulation, and there can be only very slight changes varying the magnetic field which are likely due to the depression of the energy of the two junctions of the backbone islands. We note that this comparison between the “shorted-fingers” backbone array and the backbone array embedded in the whole comb structure is a fundamental completion of the analysis reported in [14]. It is established now that the noticeable increases of the currents when the Josephson energy becomes of the order of the thermal energy is due to the “granularity” of the fingers.

3. Analysis of the Excess Voltages in Star Arrays

It is worth noting that, while the amplitude of the Josephson currents of the backbone increases noticeably, with respect to those of the reference array, as shown in Figure 4, the increased value of the gap energy does not depend on the external magnetic field. While the predictions of [11] were dealing with bosons coupling through adequate potentials, the value of the gap energy is strictly related to the condensation energy of the superconductors, and no specific predictions were made. An increased gap in our backbone structure implies an increased superconducting transition temperature, as clearly shown in [13]. This phenomenon, however, is not directly related to the topological BEC described in [11]: as we said earlier, a BEC approach of these authors relies on an existing superconducting condensate over the array, just like a BKT relies on the existence of a superfluid for vortex-antivortex dissociation. Additionally, the relative increase of the Josephson junctions of the backbone array with respect to its geometrically equivalent reference is substantially higher than the relative increases of the gaps, differently from what one would expect from the Ambegaokar-Baratoff prediction [18,20]; this statement can be clearly appreciated in Figure 3a where we see that the Josephson critical currents increase to 12% while the increase of the gaps is of the order of 3%. This phenomenon was already evident in the temperature-dependent characterizations reported in Figure 2 of [13] where one could clearly see the gap sum of the backbone array being slightly higher than the gap sum reference array, but when decreasing the temperature down to 1.2K, the increase of Josephson currents became noticeable (15%), while the gap difference remained the same. The samples in that experiment were immersed in superfluid helium, and the increase in Josephson currents could hardly be attributed to thermal effects and gradients.

Motivated by the arguments described in the previous paragraph, we decided to systematically investigate the phenomenon of the increase of the superconducting energy gap and transition temperature in graph and tree-like arrays. A recent publication, employing an approach based on the De Gennes-Alexander model [21] for granular superconductors has demonstrated that the superconducting transition temperature can be amplified in systems with specific connectivity and, in particular, star-shaped arrays of junctions [22]. In order to test the theoretical predictions of this model, we have fabricated specific samples consisting of star-graph arrays with different numbers of rays, and the CAD design of a sample with 18 rays is shown in Figure 5a (top). According to the theory, the superconducting transition temperature θ_c of a star-shaped array with p rays can be written as (see Equation (27) of [22]):

$$\theta_c = T_c \left[1 + \frac{D}{\alpha T_c} \left(\frac{p}{\sqrt{p-1}} - 2 \right) \right], \quad (1)$$

being the latter temperature amplified compared to the critical temperature T_c of a single disconnected island. Interestingly, no amplification can be observed for $p = 2$, the latter being a condition topologically equivalent to a linear array of coupled islands (like in the bottom of Figure 5a). Equation (1), depending on the coupling energy D and on the parameter α of the Ginzburg-Landau theory, suggests that the superconducting transition temperature of a star-shaped array can be enhanced by increasing the number p of rays.

Moreover, according to the BCS theory, the superconducting order parameters are related by the formula:

$$\Delta_{star} - \Delta_i \propto \left(\frac{p}{\sqrt{p-1}} - 2 \right), \tag{2}$$

with Δ_{star} and Δ_i are the superconducting gaps of the array and of the isolated island, respectively.

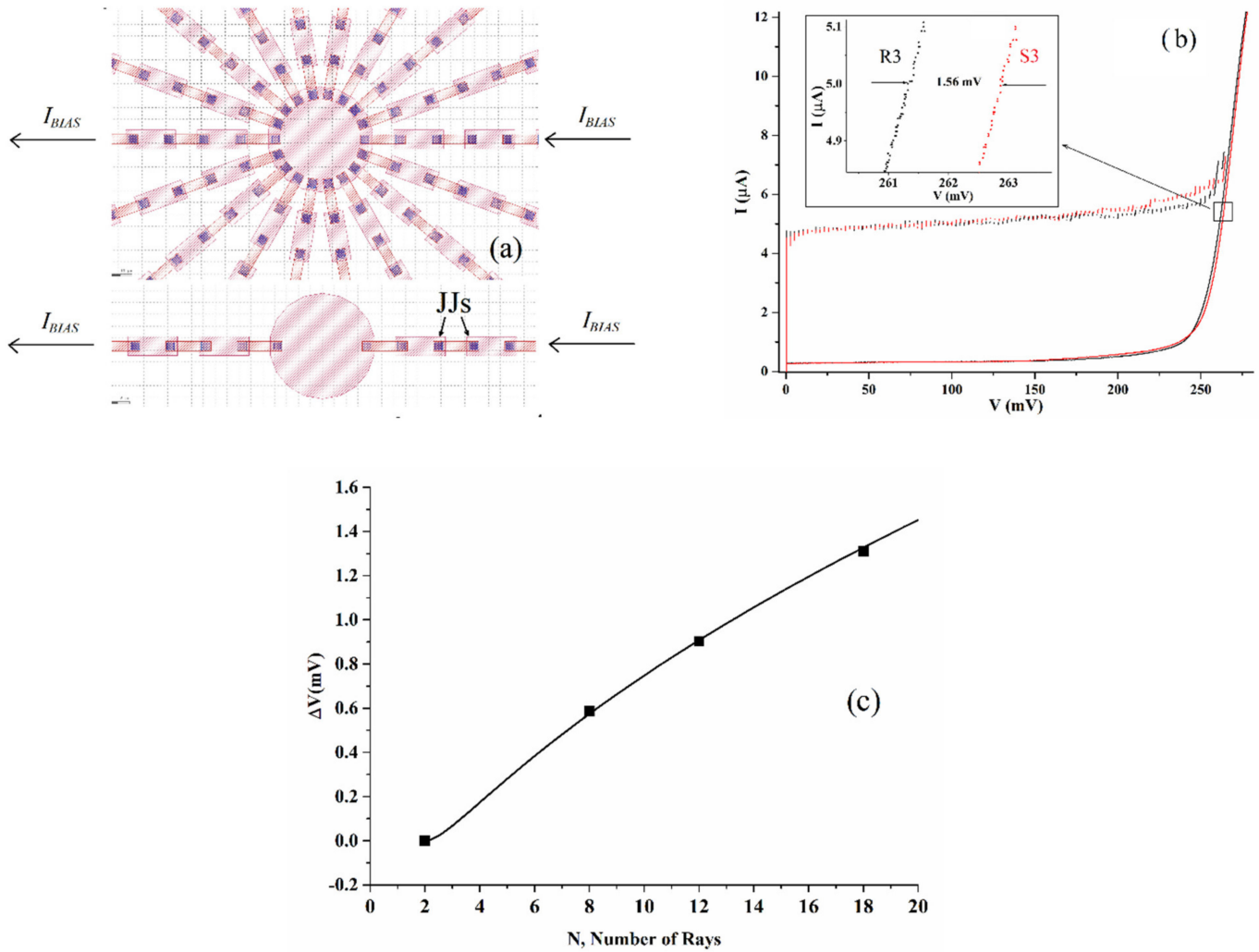


Figure 5. (a) Top: area of the central island of superconducting star-shaped arrays having 18 rays; bottom: the geometrical equivalent of two aligned rays of the star; (b) the current–voltage characteristic of two aligned rays of a star array compared with the geometrical equivalent. The inset shows a magnification of the gap region of a typical sample where S3 indicated is the star-embedded two-rays array and R3 the geometrical equivalent; (c) excess voltage of gap sum for arrays embedded in stars with an increasing number of rays. The excess voltage is measured with respect to the gap sum of two aligned “reference” rays, see (a), bottom figure. The dependence is in very good agreement with the theoretical curve obtained from a De Gennes-Alexander approach for granular superconductors (continuous curve).

We have designed star graphs having, respectively 8, 12, and 18 rays (the latter is shown in Figure 5a in the top of the figure). Each star array (103 islands and 102 junctions) had its geometrically equivalent aligned couple of rays as shown in the bottom part of Figure 5a. In Figure 5b, we show typical IV curves showing the gap-sum increase of an embedded star array, an effect better evidenced in the inset where we magnify the gap region for a star array made of 18 rays with respect to its “reference” array having only

two rays. In this case, the relative increase of the array embedded in the star graph structure, shown in the inset, is of the order of 1.35 mV at 5 μ A.

In Figure 5c, we have a plot of the increase of the gap voltage-sum for star arrays having different branches, all measured at a current of 5 μ A. The increases are all measured with respect to geometrically equivalent samples having $N = 2$ and, therefore, for $N = 2$ we have $\Delta V = 0$. Each experimental point in the plot refers to a set of four measurements performed on different days on a specific chip and the error bars would not be visible in the plot. In the figure, a comparison between experimental values and theoretical expectations is also presented. In particular, it is expected that the gap voltage-sum is described by the relation

$$\Delta V = A \left(\frac{p}{\sqrt{p-1}} - 2 \right), \quad (3)$$

which is a direct consequence of Equation (2). The full-line curve in Figure 5c is obtained by using Equation (3) with the best fit parameter $A \approx 0.56$ mV. A plot like the one shown in Figure 5c was typical for all the chips we measured. From the way the theoretical line fits our results, we conclude that the gap increase in the star graphs is consistent with a “granular” model of superconductors. As far as star graph arrays are concerned, we must specify that even the effects described in previous publications [14,15] for the increase of the Josephson currents have been observed in the present experiments. The aforementioned effect, namely the increase in the Josephson currents of several junctions, also evident in Figure 5b, was roughly the same for stars with different numbers of rays (at least the number of rays we investigated). However, it is worth pointing out that increases in Josephson currents like those shown in Figure 4 were reported in a previous publication even for star arrays [16].

We conclude this section by specifying that in the fabrication process of our samples [17] a stopping layer was deposited to prevent junctions tunnel barrier conditioning by hydrogen diffusion [23]. This technological step is a relevant support in order to ascribe unambiguously the phenomena that we observe on the Josephson critical currents and gap energies to the topological features of the samples.

4. Conclusions

Our results on graph-shaped, loopless networks of coupled superconducting islands show clear evidence of collective behavior in these systems. Some effects appear to be specific to a BEC topological condensation favored by the hopping of pairs (seen as bosons) through Josephson junctions, and this phenomenon requires the existence of a condensate. However, the superconducting condensate itself, as seen from the variations of the gap energy, is also affected by the specific network topology. We have shown that the two phenomena (noticeable increases in Josephson currents and increases in the gap voltages) are not trivially related. In the star topologies, an increasing number of rays generates an increasing excess voltage which can be well fitted by the De Gennes-Alexander theory for granular superconductors; however, the increase of the number of rays does not generate a consequent increase of the Josephson currents. It also has to be noted that the noticeable Josephson current increases observed in double comb-topology structures do not seem quantitatively relatable to the more modest excess voltages that remain constant under magnetic field and temperature variations. In conclusion, we can say that, while the Josephson currents of our structures (the pair current between the islands) is strongly influenced by the magnetic field and the temperature, the gap in excess seems to be strictly determined by the topology of the network and does not show significant changes as a function of field and temperature. Overall, our impression is that we have scratched the top of a reservoir of more intriguing phenomena involving macroscopic quantum condensates.

Author Contributions: Methodology, M.C.; design and data collection M.L. and V.M.; formal analysis and theory D.C. and F.R.; software for data acquisition and analysis V.C. and G.S.; writing and original draft preparation M.C., M.L. and F.R. All authors have read and agreed to the published version of the manuscript.

Funding: This research was funded by Istituto Nazionale di Fisica Nucleare (Italy) under grant FEEL.

Institutional Review Board Statement: Not applicable.

Data Availability Statement: Not applicable.

Acknowledgments: The first author of the paper, Massimiliano Lucci, left us, suddenly, when the manuscript had been drafted in the final form and for this reason, we kept his name in the authors list. Massimiliano approved a draft of the paper in the essentially final form. Being the first name in this list witnesses his relevant contributions.

Conflicts of Interest: The authors declare no conflict of interest.

References

1. Beasley, M.R.; Mooij, J.E.; Orlando, T.P. Possibility of Vortex-Antivortex Pair Dissociation in Two-Dimensional Superconductors. *Phys. Rev. Lett.* **1979**, *42*, 1165. [CrossRef]
2. Kosterlitz, J.M.; Thouless, D.J. Ordering, metastability and phase transitions in two-dimensional systems. *J. Phys. C Solid State Phys.* **1973**, *6*, 1181. [CrossRef]
3. Lobb, C.J.; Abraham, D.W.; Tinkham, M. Theoretical interpretation of resistive transition data from arrays of superconducting weak links. *Phys. Rev. B* **1983**, *27*, 150. [CrossRef]
4. Bednorz, J.G.; Müller, K.A. Possible high T_c superconductivity in the Ba–La–Cu–O system. *Z. Phys. B Condens. Matter* **1986**, *64*, 189. [CrossRef]
5. Prodan, J.; Migdall, A.; Phillips, W.D.; So, I.; Metcalf, H.; Dalibard, J. Stopping Atoms with Laser Light. *Phys. Rev. Lett.* **1985**, *54*, 992. [CrossRef] [PubMed]
6. Anderson, M.H.; Ensher, J.R.; Matthews, M.R.; Wieman, C.E.; Cornell, E.A. Observation of Bose-Einstein Condensation in a Dilute Atomic Vapor. *Science* **1995**, *269*, 198. [CrossRef] [PubMed]
7. Cosmic, R.; Kawabata, K.; Ashida, Y.; Ikegami, H.; Furukawa, S.; Patil, P.; Taylor, J.M.; Nakamura, Y. Probing XY phase transitions in a Josephson junction array with tunable frustration. *Phys. Rev. B* **2020**, *102*, 94509. [CrossRef]
8. Brunelli, I.; Giusiano, G.; Mancini, F.P.; Sodano, P.; Trombettoni, A. Topology-induced spatial Bose-Einstein condensation for bosons on star-shaped optical networks. *J. Phys. B At. Mol. Opt.* **2004**, *37*, S275–S286. [CrossRef]
9. Fidaleo, F. Harmonic analysis on inhomogeneous amenable networks and the Bose-Einstein condensation. *J. Stat. Phys.* **2015**, *160*, 715. [CrossRef]
10. Adami, R.; Serra, E.; Tilli, P. Negative Energy Ground States for the L2-Critical NLSE on Metric Graphs. *Commun. Math. Phys.* **2017**, *352*, 387. [CrossRef]
11. Buonsante, P.; Burioni, R.; Cassi, D.; Penna, V.; Vezzani, A. Topology-induced confined superfluidity in inhomogeneous arrays. *Phys. Rev. B* **2004**, *70*, 224510. [CrossRef]
12. Romeo, F.; De Luca, R. Cooper pairs localization in tree-like networks of superconducting islands. *Eur. Phys. J. Plus* **2022**, *137*, 726. [CrossRef]
13. Silvestrini, P.; Russo, R.; Corato, V.; Ruggiero, B.; Granata, C.; Rombetto, S.; Russo, M.; Cirillo, M.; Trombettoni, A.; Sodano, P. Topology-Induced Critical Current Enhancement in Josephson Networks. *Phys. Lett. A* **2007**, *370*, 499. [CrossRef]
14. Lucci, M.; Cassi, D.; Merlo, V.; Russo, R.; Salina, G.; Cirillo, M. Conditioning of Superconductive Properties in Graph-Shaped Reticles. *Sci. Rep.* **2020**, *10*, 10222. [CrossRef] [PubMed]
15. Lorenzo, M.; Lucci, M.; Merlo, V.; Ottaviani, I.; Salvato, M.; Cirillo, M.; Müller, F.; Weimann, T.; Castellano, M.G.; Chiarello, F.; et al. On Bose–Einstein condensation in Josephson junctions star graph arrays. *Phys. Lett. A* **2014**, *378*, 655. [CrossRef]
16. Lucci, M.; Cassi, D.; Merlo, V.; Russo, R.; Salina, G. Josephson Currents and Gap Enhancement in Graph Arrays of Superconductive Islands. *Entropy* **2021**, *23*, 811. [CrossRef]
17. Available online: https://seeqc.com/wp-content/uploads/2019/12/SeeQCSDesignRules_S1.pdf (accessed on 1 July 2019).
18. Tinkham, M. *Introduction to Superconductivity*; Dover: Mineola, NY, USA, 1996.
19. Anderson, P.W. Special Effects in Superconductivity. In *Lectures on the Many Body Problem*; Caianiello, E.R., Ed.; Academic Press: New York, NY, USA, 1964; Volume 2, pp. 113–135.
20. Ambegaokar, V.; Baratoff, A. Tunneling Between Superconductors. *Phys. Rev. Lett.* **1963**, *10*, 486. [CrossRef]
21. Berger, J.; Rubinstein, J. *Connectivity and Superconductivity*; Springer: Berlin, Germany, 2000.
22. Romeo, F. Order parameter focalization and critical temperature enhancement in synthetic networks of superconducting islands. *J. Phys. Condens. Matter* **2021**, *33*, 45401. [CrossRef]
23. Tolpygo, S.K.; Amparo, D.; Hunt, R.T.; Vivalda, J.A.; Johannes, D.T. Diffusion Stop-Layers for Superconducting Integrated Circuits and Qubits with Nb-based Josephson Junctions. *IEEE Trans. Appl. Supercond.* **2010**, *21*, 119. [CrossRef]